Muse cells decrease the neuroinflammatory response by modulating the proportion of M1 and M2 microglia *in vitro*

Xin-Yao Yin[1], Chen-Chun Wang[1], Pan Du[1], Xue-Song Wang[2], Yi-Chi Lu[1], Yun-Wei Sun[1], Yue-Hui Sun[1], Yi-Man Hu[1], Xue Chen[1,*]

https://doi.org/10.4103/1673-5374.343885

Date of submission: September 9, 2021

Date of decision: November 26, 2021

Date of acceptance: December 3, 2021

Date of web publication: April 25, 2022

From the Contents

Graphical Abstract

Muse cells decrease the number of M1 microglia and increase the proportion of M2 microglia when cocultured with lipopolysaccharide-stimulated microglia

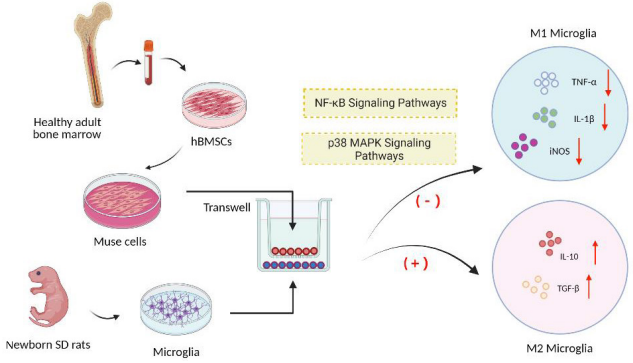

Abstract

Neuroinflammation hinders repair of the central nervous system (CNS). Stem cell transplantation is a very promising approach for treatment of CNS injuries. However, it is difficult to select seed cells that can both facilitate nerve regeneration and improve the microenvironment in the CNS. In this study, we isolated multilineage-differentiating stress-enduring (Muse) cells from bone marrow mesenchymal stem cells. We explored the anti-inflammatory effect and mechanism of Muse cells *in vitro* by coculture of Muse cells with lipopolysaccharide-stimulated microglia. Our results showed that Muse cells effectively reduced the transcription and secretion of tumor necrosis factor α and interleukin-1β and increased the expression of transforming growth factor-β and interleukin-10 in microglia. In addition, Muse cells decreased the number of M1 microglia and increased the proportion of M2 microglia in an inflammatory environment more effectively than bone marrow mesenchymal stem cells. We also show that Muse cells inhibited the protein expression of toll-like receptor 4 (TLR4) and myeloid differentiation primary response protein (MyD88) and inhibited the expression of the phosphorylated forms of transcription factor p65, nuclear factor (NF)-κB inhibitor alpha, and p38 mitogen-activated protein kinase (MAPK) in microglia. Therefore, we suggest Muse cells cause antineuroinflammatory effects by inhibition of the TLR4/MyD88/NF-κB and p38 MAPK signaling pathways in microglia. Our results shed light on the function of Muse cells in relation to CNS diseases and provide insight into the selection of seed cells.

Key Words: bone marrow mesenchymal stem cells; central nervous system; lipopolysaccharide; multilineage-differentiating stress-enduring cells; neuroinflammation; microglia; signaling pathway

Introduction

Neuroinflammation is an important pathological process that mediates various types of central nervous system (CNS) injuries and diseases (Yang et al., 2019; Mithaiwala et al., 2021). Microglia are the main resident immune cells in the CNS; they constantly regulate the microenvironment and secrete factors that affect surrounding cells (Colonna et al., 2017). Microglia play different roles in CNS diseases depending on their phenotype. M1 microglia secrete proinflammatory mediators such as tumor necrosis factor α (TNF-α), interleukin (IL)-1β, and nitric oxide, thereby aggravating the CNS inflammatory response after injury. M2 microglia, in contrast, secrete IL-4, IL-10, and other factors that promote the repair of nerve damage and produce neuroprotective effects (Ransohoff, 2016; Tang et al., 2016; Kobashi et al., 2020). Recently, many studies have focused on reducing CNS damage and promoting nerve-tissue repair by regulating the phenotype of microglia (Bassett et al., 2021; Wu et al., 2021; Zhou et al., 2021b). These mechanistic studies have found that the nuclear factor (NF)-κB and mitogen-activated protein kinase (MAPK) signaling pathways are the two most important pathways that regulate the inflammatory activity of microglia (Singh et al., 2020; Zhang et al., 2021). Therefore, therapeutic approaches targeting these two pathways are effective means of improving the inflammatory microenvironment after CNS injury (Xu et al., 2020; Tang et al., 2021; Yang et al., 2021).

Stem cell transplantation has recently led to remarkable improvements after CNS injury; however, selection of seed cells remains a challenge. Finding cells that can both differentiate into neural tissue and improve the microenvironment at a CNS injury site has become a major research focus. To date, bone marrow mesenchymal stem cells (BMSCs) have been used in many trials to treat CNS disease (Hu et al., 2021; Sun et al., 2021). BMSCs can differentiate into neuronal cells at a CNS injury site, thus replenishing the loss of neuronal cells (Zhan et al., 2020; Li et al., 2021). BMSCs can also foster recovery after injury and alleviate inflammation owing to paracrine effects (Luo et al., 2021). Nevertheless, the low cell-survival rate and limited level of differentiation to neural tissue after *in vivo* transplantation of BMSCs are problems that restrict their application (Lin et al., 2020).

Multilineage-differentiating stress-enduring (Muse) cells are a new type of pluripotent stem cell discovered in 2010 that can be obtained from dermal tissue, adipose tissue, and mesenchymal tissue. Muse cells are stress-tolerant and can differentiate into cell types corresponding to the three germ layers without immune rejection when implanted *in vivo* (Kuroda et al., 2010). Recently, Muse cells were used clinically to treat spinal cord injury and some CNS diseases (Dezawa, 2018). Recent studies have found that Muse cells have a high survival rate at the injured site and can differentiate into and integrate with surrounding injured cells in large quantities (Iseki et al., 2017; Yamada

[1]Department of Basic Medicine, Wuxi School of Medicine, Jiangnan University, Wuxi, Jiangsu Province, China; [2]Department of Orthopedics, Affiliated Hospital of Jiangnan University, Wuxi, Jiangsu Province, China

*Correspondence to: Xue Chen, PhD, snow@jiangnan.edu.cn.

https://orcid.org/0000-0003-4766-232X (Xue Chen)

Funding: *The study was supported by the National Natural Science Foundation of China, No. 81501610 (to XC); a grant for Development of Science and Technology of Wuxi, Nos. N20202030 (to XC), N20192025 (to XSW); Postgraduate Research & Practice Innovation Program of Jiangsu Province, No. KYCX20_1960 (to XYY).*

How to cite this article: *Yin XY, Wang CC, Du P, Wang XS, Lu YC, Sun YW, Sun YH, Hu YM, Chen X (2023) Muse cells decrease the neuroinflammatory response by modulating the proportion of M1 and M2 microglia in vitro. Neural Regen Res 18(1):213-218.*

et al., 2018; Kajitani et al., 2021). In addition, Muse cells are potentially anti-inflammatory. Gimeno et al. (2017) found that Muse cells can secrete a large amount of transforming growth factor (TGF)-β1, which improved the inflammatory response in diabetic mice. Suzuki et al. (2021) discovered that Muse cells can reduce mRNA expression of TNF-α and inducible nitric oxide synthase (iNOS) in microglia. However, it has yet to be established whether Muse cells can regulate M1/M2 microglia expression in a neuroinflammatory microenvironment and what the associated mechanism of action would be.

Therefore, in this study, we cocultured Muse cells with lipopolysaccharide (LPS)-stimulated microglia to explore their anti-inflammatory capacity, to discover anti-inflammatory differences with BMSCs, and to determine the possible mechanisms involved, so as to provide a basis for further application of Muse cells in the treatment of CNS injuries and diseases.

Methods

Cells

Healthy human adult bone marrow used in this study was provided by the Department of Orthopedics, Affiliated Hospital of Jiangnan University, China, with informed consent. The study was approved by the Ethics Committee of Jiangnan University on January 3, 2019 (No. 2019-037) and conducted in accordance with the 1964 *Declaration of Helsinki*, as revised in 2013. BMSCs were isolated from human bone marrow by a density-gradient method as described previously (Shichinohe et al., 2011) and cultured in Dulbecco's Modified Eagle Medium (DMEM; Thermo Fisher Scientific, Waltham, MA, USA, Cat# 10567014) containing 15% fetal bovine serum (FBS; Thermo Fisher Scientific).

BMSCs at passage 4 were collected and incubated with 0.25% trypsin (Thermo Fisher Scientific) at 37°C for 8 hours. The cells at a cell density of 1×10^4/mL were plated in ultra-low-attachment 6-well cell culture dishes (Corning Inc., Corning, NY, USA, Cat# 3471) and incubated in Minimum Essential Medium α (α-MEM; Thermo Fisher Scientific) containing 20% FBS and 0.9% MethoCult H4100 (STEMCELL Technologies Canada Inc., Vancouver, Canada, Cat# 04100) at 37°C with 5% CO_2. Muse cell spheres were collected after 3 to 5 days of culturing and then inoculated into 10 cm^2 culture dishes for adherent cell culture. Each passage alternated between suspension and adherent culture (Kuroda et al., 2010).

Primary rat microglia were isolated from the brains of 1-day-old newborn Sprague-Dawley (SD) rats as reported (Fu et al., 2017). Briefly, newborn SD rats were anesthetized with 2% isoflurane (Shanghai Yuyan Scientific Instrument Co., Ltd., Shanghai, China) in oxygen for 2 minutes via inhalation, sterilized with 75% alcohol, and placed on an ultraclean table. The extracerebral skin was cut, the skull was lifted, and the brain was removed into phosphate-buffered saline (PBS). The meninges and blood vessels were removed from the brain, and the remaining brain tissue was homogenized and then digested at 37°C for 15–20 minutes with trypsin (Thermo Fisher Scientific). FBS was added, the samples were centrifuged at 400 × *g* for 5 minutes, and the cells from the pellet were cultured in an incubator at 37°C and 5% CO_2. Once the cells were 90% confluent, they were shaken at 20 × *g* for 1 hour. The medium was collected and centrifuged at 400 × *g* for 5 minutes. DMEM/F12 medium (Thermo Fisher Scientific) containing 10% FBS was used to culture the primary rat microglia in T25 culture flasks (Corning Inc.).

Transwell coculture

To explore the role of Muse cells on microglia in an inflammatory environment, primary rat microglia were randomly divided into several groups. (1) Control group: microglia (1×10^6/mL) were cultured in DMEM/F12 medium for 24 hours; (2) LPS group: microglia (1×10^6/mL) were cultured in DMEM/F12 medium containing 1 μg/mL LPS (MilliporeSigma, Burlington, MA, USA, Cat# L6529) for 24 hours; (3) BMSC group: microglia (1×10^6/mL) were cocultured with BMSCs (1×10^5/mL) in DMEM/F12 medium containing 1 μg/mL LPS for 24 hours; and (4) Muse group: microglia (1×10^6/mL) were cocultured with Muse cells (1×10^5/mL) in DMEM/F12 medium containing 1 μg/mL LPS for 24 hours. Next, the microglia were extracted for use in quantitative reverse transcription-polymerase chain reaction, enzyme-linked immunosorbent assay (ELISA), flow cytometry, and western blot assay.

Stem cells were cocultured with microglia as follows: Muse cells or BMSCs (1×10^5/mL) were seeded in 0.4-μm inserts from transwell plates (Corning Inc., Cat# 3412) and the inserts were placed on a sterile six-well plate. Microglia were plated on the bottom of the transwell plate at a cell density of 1×10^6/mL. After 24 hours, both stem cells and microglia had adhered to the walls and bottom of the inserts. The cells were washed twice with PBS and were cocultured by placing the insert of the transwell, containing Muse cells or BMSCs, above the lower chamber of the transwell that contained microglia.
To investigate the mechanism of action of Muse cells, microglia were divided randomly into four groups. (1) Control group: microglia (1×10^6/mL) were cultured in DMEM/F12 medium for 2 hours; (2) Muse coculture group: microglia (1×10^6/mL) were cocultured with Muse cells (1×10^5/mL) in DMEM/F12 medium for 2 hours; (3) LPS group: microglia (1×10^6/mL) were cultured in DMEM/F12 medium containing 1 μg/mL LPS for 2 hours; and (4) Muse coculture + LPS group: microglia (1×10^6/mL) were cocultured with Muse cells (1×10^5/mL) in DMEM/F12 medium containing 1 μg/mL LPS for 2 hours. The coculture procedure was the same as described above. After coculture, microglia were extracted for western blot assay.

Immunocytochemistry

As Muse cells stain positive by immunocytochemistry for both stage-specific embryonic antigen-3 (SSEA-3) and endoglin (CD105) (Uchida et al., 2016), the following immunocytochemistry method was used to identify our acquired cells. Established Muse cell spheres at passage 3 were aspirated and fixed with 4% paraformaldehyde for 30 minutes. After washing three times with PBS, the cells were blocked with 0.5% bovine serum albumin for 1 hour and then incubated with rat anti-SSEA-3 (1:200, Thermo Fisher Scientific, Cat# 14-8833-80, RRID: AB_657839) and rabbit anti-CD105 (1:200, Abcam, Cambridge, UK, Cat# ab107595, RRID: AB_10863525) antibodies at 4°C overnight. After washing three times with PBS containing 0.1% Tween 20, Muse cell spheres were incubated with Alexa Fluor® 647-labeled goat anti-rat secondary antibody (1:200, Abcam, Cat# ab150167, RRID: AB_2864291) and FITC-labeled goat anti-rabbit secondary antibody (1:200, Abcam, Cat# ab6717, RRID: AB_955238) separately for 1.5 hours at room temperature. Hoechst 33342 (Beyotime Biotechnology, Shanghai, China, Cat# C1025) was used in the dark for 3 minutes to stain the cell nuclei. Images were captured with a laser confocal microscope (LSM 880, ZEISS, Oberkochen, Germany).

We used immunocytochemistry to identify the purity of the extracted primary microglia according to the integrin alpha-M (CD11b)-positive characteristics of microglia. Briefly, cells were fixed in 4% paraformaldehyde for 15 minutes, washed three times in PBS, and incubated in 0.5% bovine serum albumin for 1 hour, followed by incubation with rabbit anti-mouse CD11b antibody (1:200, Abcam, Cat# ab184308, RRID: AB_2889154) at 4°C overnight. Next, cells were washed with PBS containing 0.1% Tween 20, incubated with Alexa Fluor® 555-labeled goat anti-rabbit secondary antibody (1:200, Abcam, Cat# ab150078, RRID: AB_2722519) for 1.5 hours at room temperature, and nuclei were stained with Hoechst 33342 for 3 minutes. Images were captured with a laser confocal microscope (LSM 880, ZEISS).

Quantitative reverse transcription-polymerase chain reaction

We used quantitative reverse transcription-polymerase chain reaction to analyze the transcript levels of inflammation-related genes in microglia; we examined the mRNA expression of the proinflammatory factors TNF-α, IL-1β, and iNOS and the anti-inflammatory factors TGF-β and arginase-1 (Arg-1). After coculture for 24 hours, we extracted total RNA from microglia using the RNA-Quick Purification Kit (Shanghai Yishan Biotechnology Co., Shanghai, China, Cat# ES-RN001) and converted total RNA to cDNA using the PrimeScript™ RT Master Mix (Takara Bio Inc., Kusatsu, Japan, Cat# RR036A). Quantitative reverse transcription-polymerase chain reaction was performed on a LightCycler 480 II (Roche, Basel, Switzerland) using TB Green® Premix Ex Taq™ II (Takara Bio Inc., Cat# RR820A). Glyceraldehyde-3-phosphate dehydrogenase (GAPDH) was used to normalize the gene expression, and the $2^{-\Delta\Delta Ct}$ method (Livak et al., 2001) was employed to calculate the relative quantity of mRNA. The polymerase chain reaction conditions were 95°C for 30 seconds, followed by 95°C for 5 seconds, 55°C for 30 seconds, and 72°C for 30 seconds, with 40 cycles. Primer sequences were designed and synthesized by Sangon Biotech (Shanghai) Co., (Shanghai, China) and are shown in **Table 1**.

Table 1 | **Primers used for quantitative reverse transcription-polymerase chain reaction**

Gene	Sequences (5'–3')	Product size (bp)
TNF-α	Forward: ACT GAA CTT CGG GGT GAT CG	153
	Reverse: GCT TGG TGG TTT GCT ACG AC	
IL-1β	Forward: CTC ACA GCA GCA TCT CGA CAA GAG	95
	Reverse: TCC ACG GGC AAG ACA TAG GTA GC	
Arg-1	Forward: AGT GTG GTG CTG GGT GGA GAC	118
	Reverse: GCG GAG TGT TGA TGT CAG TGT GAG	
TGF-β	Forward: GAC CGC AAC AAC GCA ATC TATG AC	94
	Reverse: CTG GCA CTG CTT CCC GAA TGT C	
iNOS	Forward: TCT TGG AGC GAG TTG TGG ATT GTT C	146
	Reverse: AGT GAT GTC CAG GAA GTA GGT GAG G	
GAPDH	Forward: TCC TGG AAG ATG GTG ATG GGT T	224
	Reverse: AAG GTC GGT GTG AAC GGA TTT GG	

GAPDH: Glyceraldehyde-3-phosphate dehydrogenase; IL-1β: interleukin-1β; iNOS: inducible nitric oxide synthase; TGF: transforming growth factor; TNF: tumor necrosis factor.

Enzyme-linked immunosorbent assay

We investigated the levels of inflammation-related factors released from microglia by assaying the proinflammatory factors TNF-α and IL-1β and the anti-inflammatory factor IL-10 by ELISA. After coculture for 24 hours, we detected separately the levels of TNF-α, IL-1β, and IL-10 in supernatants of microglia using the rat TNF-α ELISA kit (Signalway Antibody LLC, Nanjing, China, Cat# EK17664), the rat IL-1β ELISA kit (Signalway Antibody LLC, Cat# EK14826), and the rat IL-10 ELISA kit (Cat# BE45311, IBL International GmbH, Hamburg, Germany) in accordance with the manufacturers' instructions.

Flow cytometry

As iNOS is a key marker of M1 microglia, we detected iNOS-positive microglia to confirm the number of M1 microglia in each group. Microglia were collected and fixed in Fixation Buffer (BioLegend, San Diego, CA, USA, Cat# 420801) for 30 minutes. After washing with PBS three times,

the cells were incubated with 1× Intracellular Staining Permeabilization Wash Buffer (BioLegend, Cat# 421002) containing Alexa Fluor® 488-labeled iNOS antibody (0.06 μg/100 μL, Thermo Fisher Scientific, Cat# 53-5920-82, RRID: AB_2574423) for 30 minutes at 4°C protected from light. Finally, cells were washed three times with PBS and detected using a BD Accuri C6 flow cytometer (BD Biosciences, Franklin Lakes, NJ, USA). Data were analyzed using FlowJo™ Software Version 10 (Becton, Dickinson and Company, 2019, Ashland, OR, USA).

Western blot assay

To detect the presence of M2 microglia in our isolated primary microglia, we measured the protein levels of the M2 microglia marker macrophage mannose receptor 1 (CD206). In addition, to investigate whether nuclear factor-κB (NF-κB) and MAPK pathways, the major signaling pathways of microglial inflammatory response, were regulated by Muse cells, we examined the key proteins in the pathways such as toll-like receptor 4 (TLR4), myeloid differentiation primary response protein (MyD88), transcription factor p65, phosphorylated p65 (p-p65), nuclear factor-κB inhibitor alpha (IκBα), phosphorylated IκBα (p-IκBα), JNK, phosphorylated JNK (p-JNK), ERK, phosphorylated ERK (p-ERK), p38 mitogen-activated protein kinase, and phosphorylated p38 mitogen-activated protein kinase (p-p38). Primary microglia were washed with cold PBS and collected in RIPA buffer (Beyotime Biotechnology) with 1% (v/v) EZBlock™ Protease Inhibitor Cocktail, EDTA-Free (BioVision Inc., Milpitas, CA, USA, Cat# K272-5) and 1% (v/v) Phosphatase Inhibitor Cocktail 2 (MilliporeSigma, Cat# P5726). After sonication, the cells were centrifuged at 8000 × *g* at 4°C for 10 minutes. The total protein concentration was determined using a BCA protein assay kit (Beyotime Biotechnology, Cat# P0012). Next, the proteins were separated by 10% sodium dodecyl sulfate-polyacrylamide gel electrophoresis and then transferred onto polyvinylidene fluoride membranes (Bio-Rad Laboratories, Hercules, CA, USA). The membranes were blocked with QuickBlock™ western blocking buffer (Beyotime Biotechnology, Cat# P0252) for 1 hour and then incubated with the following primary antibodies: rabbit anti-CD206 (1:500, Abcam, Cat# ab64693, RRID: AB_1523910), mouse anti-GAPDH (1:5000, Abcam, Cat# ab8245, RRID: AB_2107448), rabbit anti-NF-κB p65 (1:2000, Abcam, Cat# ab16502, RRID: AB_443394), rabbit anti-NF-κB p65 (phospho S536) (1:1000, Abcam, Cat# ab86299, RRID: AB_1925243), rabbit anti-IκBα (1:1000, Abcam, Cat# ab32518, RRID: AB_733068), rabbit anti-IκBα (phospho S32) (1:1000, Cell Signaling Technology, Danvers, MA, USA, Cat# 2859, RRID: AB_561111), rabbit anti-TLR4 (1:500, Proteintech Group Inc., Rosemont, IL, USA, Cat# 19811-1-AP, RRID: AB_10638446), rabbit anti-MyD88 (1:1000, Abcam, Cat# ab219413), rabbit anti-p38 (1:1000, Abcam, Cat# ab170099), rabbit anti-p38 MAPK (phospho Thr180/Tyr182) (1:1000, Cell Signaling Technology, Cat# 4511, RRID: AB_2139682), rabbit anti-ERK1 + ERK2 (1:1000, Abcam, Cat# ab184699, RRID: AB_2802136), rabbit anti-ERK1 (phospho T202) + ERK2 (phospho T185) (1:1000, Abcam, Cat# ab201015), rabbit anti-JNK1 + JNK2 + JNK3 (1:1000, Abcam, Cat# ab179461, RRID: AB_2744672), rabbit anti-JNK1 (phospho Y185) + JNK2 (phospho Y185) + JNK3 (phospho Y223) (1:1000, Abcam, Cat# ab76572, RRID: AB_1523840) overnight at 4°C. Next, the blots were incubated with the corresponding secondary antibodies horseradish peroxidase (HRP)-conjugated goat anti-rabbit IgG (1:20,000, Shanghai Yishan Biotechnology Co., Cat# SGARHRP) and HRP-conjugated goat anti-mouse IgG (1:20,000, Shanghai Yishan Biotechnology Co., Cat# SGAMHRP) for 2 hours at room temperature. Membrane exposure was performed with a chemiluminescent detection kit (Thermo Fisher Scientific, Cat# 34580) using the ChemiDoc™ MP Imaging System (Universal Hood III, Bio-Rad Laboratories). The grayscale value of each protein was obtained using ImageJ software v1.52 (National Institutes of Health, Bethesda, MD, USA; Schneider et al., 2012). Relative protein expression was normalized to GAPDH.

Statistical analysis

All data are shown as the mean ± the standard error of the mean. Multiple group comparisons were analyzed using one-way analysis of variance followed by Tukey's *post hoc* tests. Statistical analyses were performed using GraphPad Prism 8.0 (GraphPad Software, San Diego, CA, USA, www.graphpad.com) and analyzed using SPSS 20 software (IBM, Armonk, NY, USA). We set the level at which differences were statistically significant to $P < 0.05$.

Results

The morphology and characteristics of Muse cells

When Muse cells were cultured in suspension for 5 to 7 days, the cells were seen to aggregate into cell colonies (**Figure 1A**). Muse cells were then collected, digested with trypsin to single cells, and inoculated in adherent culture dishes. After 1 day, the cells adhered to the walls and began to divide and proliferate (**Figure 1B**). Muse cell bodies are slightly smaller than BMSCs, but they are also spindle-shaped and have similar morphology to BMSCs. The expression of markers was detected in cell spheres using immunocytochemistry; the cells were positive for both the pluripotent stem cell marker SSEA-3 and the mesenchymal stem cell marker CD105 (**Figure 1C–E**), which is consistent with the characteristics of Muse cells.

Muse cells affect levels of proinflammatory TNF-α and IL-1β and anti-inflammatory TGF-β and IL-10 in coculture

The purity of the extracted primary microglia was over 90% as identified by immunocytochemistry (**Additional Figure 1**). To explore whether the Muse cells influenced inflammatory cytokine production, cytokine transcription levels were measured in microglia after 24 hours of coculture. Compared with those in the control group, the proinflammatory factors TNF-α and IL-1β were significantly upregulated and the anti-inflammatory factor TGF-β was significantly downregulated in the LPS group ($P < 0.001$; **Figure 2A–C**). The expression levels of TNF-α and IL-1β were significantly decreased in both stem cell coculture groups compared with those in the LPS group ($P < 0.001$ for both; **Figure 2A** and **B**) and in the Muse cell group compared with those in the BMSC group ($P < 0.01$ and $P < 0.05$, respectively; **Figure 2A** and **B**). Meanwhile, Muse cells had upregulated expression of TGF-β compared with that in the control group ($P < 0.01$; **Figure 2C**), although there was no statistical difference compared with BMSCs.

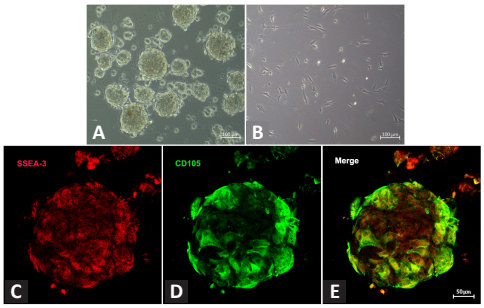

Figure 1 | **Culture and identification of Muse cells.**
(A) Muse cells become spheres after 5–7 days of suspension culture, as observed under light microscopy. (B) The morphology of Muse cells in adherent culture, as observed under light microscopy. (C–E) Muse cells were positive for SSEA-3 (red) and CD105 (green). Scale bars: 100 μm in A and B; 50 μm in C–E. SSEA-3: Stage-specific embryonic antigen-3.

As inflammatory factors secreted by microglia have a great impact on surrounding cells and tissues, we investigated the effect of Muse cells on the release of inflammatory cytokines from microglia. There was a significant increase in the secretion of the proinflammatory factors TNF-α and IL-1β in microglia in the LPS group compared with that in the control group (**Figure 2D** and **E**), while the production levels of these two factors were statistically significantly reduced after coculture of microglia with Muse cells or BMSCs ($P < 0.001$; **Figure 2D** and **E**). In particular, TNF-α expression was significantly decreased in the Muse cell group compared with that in the BMSC group ($P < 0.05$; **Figure 2D**). However, there was no statistical difference in IL-1β secretion between the BMSC and Muse cell groups (**Figure 2E**). At the same time, IL-10 secreted by microglia in the LPS group was increased relative to the control group (**Figure 2F**) and was even higher in both stem cell groups relative to the control group. In particular, in the Muse cell group, IL-10 secretion was nearly twice that of the LPS group and was also significantly different from the BMSC coculture group ($P < 0.05$; **Figure 2F**).

Muse cells change the ratio of M1/M2 microglia in the inflammatory environment

We detected microglial phenotypic changes by analyzing expression of markers specific to M1 and M2 microglia. In our study, flow cytometry results showed that the number of iNOS-positive M1 cells was significantly higher in the LPS group compared with that in the control group. The presence of Muse cells strongly reduced the number of M1 microglia compared with that in the LPS group ($P < 0.001$), an effect that was more obvious than that of BMSCs ($P < 0.01$; **Figure 3A–E**). These results agree with the mRNA expression levels of iNOS (**Figure 3H**). Western blot assay also showed that the protein expression of the M2 marker CD206 in the LPS group was significantly lower than that in the control group ($P < 0.01$) and in the Muse cell group ($P < 0.05$), but there was no significant difference between the LPS group and the BMSC group (**Figure 3F** and **G**). The transcript levels of another M2 marker, Arg-1, was also greatly increased by Muse cells; Arg-1 expression levels reached three times that of the LPS group and far exceeded that of the BMSC group ($P < 0.001$; **Figure 3I**). Combined, these results indicate that Muse cells can lower the number of M1 microglia and increase the proportion of M2 microglia in an inflammatory microenvironment.

Muse cells exert antineuroinflammatory effects by regulating TLR4/MyD88/NF-κB and p38 MAPK signaling pathways in microglia

NF-κB and MAPK signaling pathways are important for microglial activation. We tested the expression of key proteins in the NF-κB and MAPK signaling pathways after coculturing Muse cells with primary microglia in normal medium; we found the expression levels of the key proteins were similar to that of the control group (**Figure 4A–D**). When microglia were cultured in medium containing 1 μg/mL LPS for 2 hours, we detected a clear rise in the expression of both TLR4 and MyD88 (**Figure 4A** and **B**). In parallel, we detected upregulation of the phosphorylation levels of p65, IκBα, p38, ERK, and JNK (**Figure 4**), suggesting that the NF-κB and MAPK signaling pathways were activated by LPS in microglia. When Muse cells were cocultured with microglia in LPS-containing medium, Muse cells downregulated the expression of TLR4 ($P < 0.05$) and MyD88 ($P < 0.05$) in microglia and significantly inhibited the phosphorylation levels of p65 ($P < 0.001$) and IκBα ($P < 0.05$; **Figure 4A** and **B**), indicating that Muse cells suppressed the TLR4/MyD88/NF-κB signaling pathway. In contrast, Muse cells also downregulated the phosphorylation level of p38 in microglia, but we observed no significant changes in the phosphorylation expression of ERK and JNK, demonstrating that Muse cells could inhibit the activation of the p38 MAPK signaling pathway in microglia (**Figure 4C** and **D**).

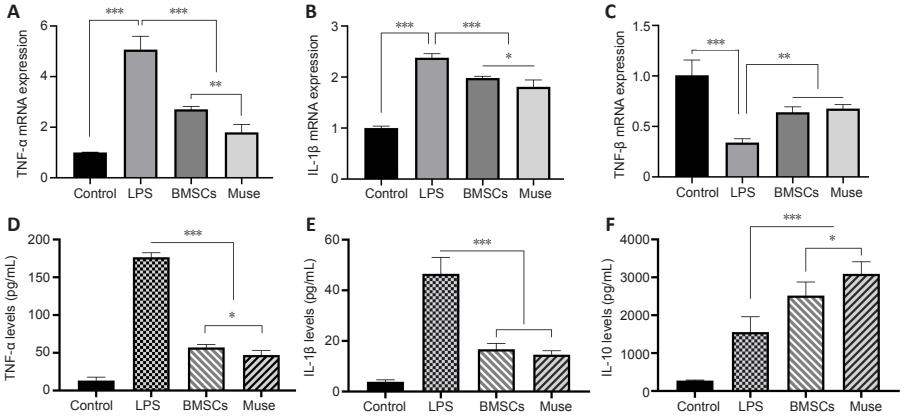

Figure 2 | **Synthesis and expression of inflammatory factors in microglia.**
(A–C) mRNA expression of TNF-α (A), IL-1β (B), and TGF-β (C) in microglia, measured by quantitative reverse transcription-polymerase chain reaction. Data are expressed as the mean ± SEM (n = 3). (D–F) The secretion of TNF-α (D), IL-1β (E), and IL-10 (F) in microglia measured by enzyme-linked immunosorbent assay. Data are shown as the mean ± SEM (n = 6). *P < 0.05, **P < 0.01, ***P < 0.001 (one-way analysis of variance followed by Tukey's *post hoc* tests). BMSCs: Bone marrow mesenchymal stem cells; IL: interleukin; LPS: lipopolysaccharide; SEM: standard error of the mean; TGF: transforming growth factor; TNF: tumor necrosis factor.

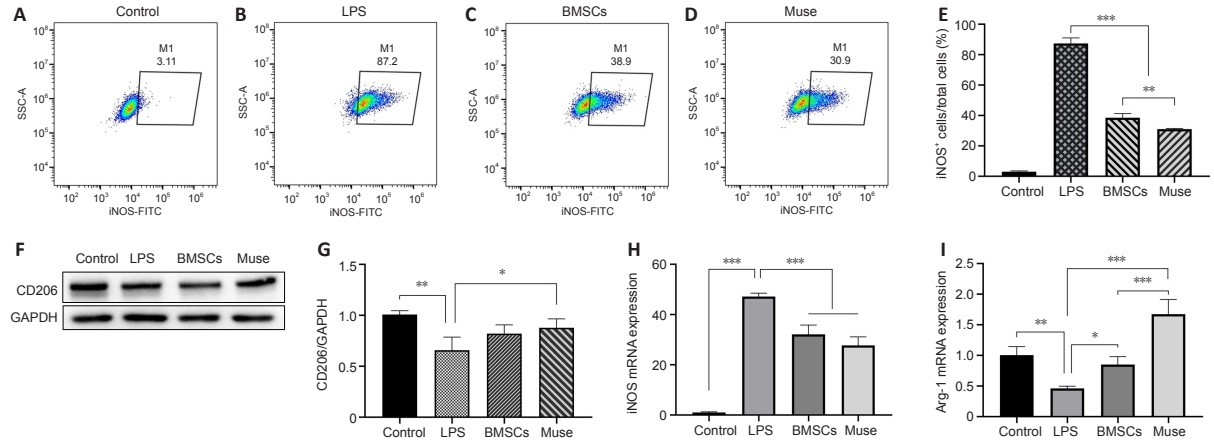

Figure 3 | **The M1/M2 phenotypic changes of microglia.**
(A–D) The proportion of iNOS-positive cells (M1-type cells) in the control (A), LPS (B), BMSC (C), and Muse cell groups (D) measured by flow cytometry. The quantitative data are shown in E. CD206 protein expression was detected by western blotting for each group, and the corresponding quantitative data are shown in G. (H, I) mRNA levels of iNOS (H) and Arg-1 (I) measured by quantitative reverse transcription-polymerase chain reaction. Data are shown as the mean ± SEM (n = 3). *P < 0.05, **P < 0.01, ***P < 0.001 (one-way analysis of variance followed by Tukey's *post hoc* tests). Arg-1: arginase-1; BMSCs: bone marrow mesenchymal stem cells; GAPDH: glyceraldehyde-3-phosphate dehydrogenase; iNOS: inducible nitric oxide synthase; LPS: lipopolysaccharide; SEM: standard error of the mean.

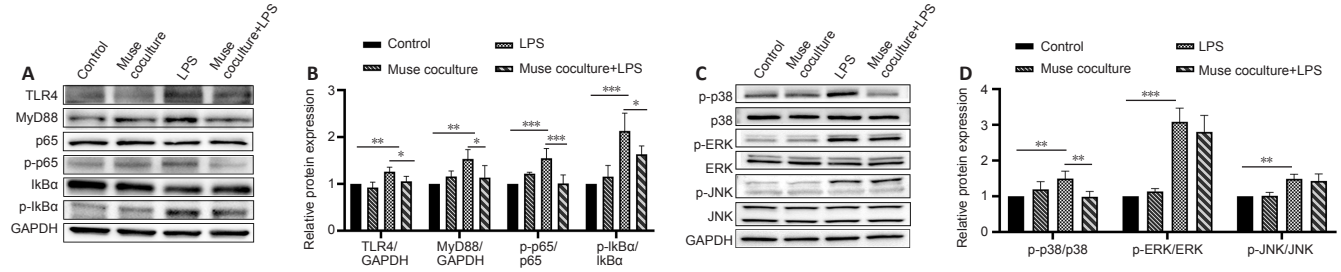

Figure 4 | **Protein expression of NF-κB and MAPK signaling pathway in microglia.**
(A) Representative western blot of TLR4, MyD88, p65, p-p65, IκBα, and p-IκBα expression and (B) the quantitative analysis of protein expression. (C) Representative western blot of p-p38, p38, p-ERK, ERK, p-JNK, and JNK expression in microglia and (D) the quantitative analysis of protein expression. The protein expression levels are relative to the control group (set to a relative protein expression value of 1). Data are shown as the mean ± SEM (n = 3). *P < 0.05, **P < 0.01, ***P < 0.001 (one-way analysis of variance followed by Tukey's *post hoc* tests). GAPDH: Glyceraldehyde-3-phosphate dehydrogenase; IκBα: nuclear factor-κB inhibitor alpha; LPS: lipopolysaccharide; MAPK: mitogen-activated protein kinase; MyD88: myeloid differentiation primary response protein MyD88; NF-κB: nuclear factor-κB; p38: p38 mitogen-activated protein kinase; p65: transcription factor p65; p-p65: phosphorylated transcription factor p65; p-p38: phosphorylated p38 mitogen-activated protein kinase; p-ERK: phosphorylated ERK; p-IκBα: phosphorylated nuclear factor-κB inhibitor alpha; p-JNK: phosphorylated JNK; SEM: standard error of the mean; TLR4: toll-like receptor 4.

Discussion

The immense loss of nerve cells and their ineffective replenishment is a challenge when repairing the CNS after injury (Fawcett, 2020), making it difficult to regenerate injured neural tissue. The inflammatory response in the microenvironment surrounding the injury exacerbates apoptosis at the injury site, making the injury persistent. Nowadays, stem cell therapy for treatment of CNS diseases is an effective tool; mesenchymal stem cells (MSCs) are one of the most widely used stem cell types (Lo Furno et al., 2018), of which BMSCs are the most commonly used. *In vivo* transplantation of BMSCs has been confirmed to improve motor function in CNS-injured animals (Xiong et al., 2017); however, the percentage of BMSCs that differentiate into neural tissue was found to be extremely low, and the BMSCs had a poor survival rate (Neirinckx et al., 2014). Therefore, current research efforts are dedicated to overcome the deficiencies of BMSCs in CNS treatment by using exosomes secreted by BMSCs (Liu et al., 2019), by preconditioning BMSCs with stromal cell-derived factor 1α or hypoxic conditions (Yu et al., 2016; Beigi Boroujeni et al., 2020), or by using tissue-engineering scaffolds (Luo et al., 2021). In this study, we used BMSC-derived Muse cells, a new type of pluripotent stem cell that are stress-tolerant and express pluripotent stem cell markers such as SSEA-3, octamer-binding protein 3/4 (OCT3/4), transcription factor SOX-2, homeobox protein NANOG, and mesenchymal stem cell markers such as CD105. We treated BMSCs with trypsin for 8 hours as previously reported (Kuroda et al., 2010). The surviving cells stained positive for SSEA-3 and CD105 by immunocytochemistry, thus confirming they were Muse cells. Increasing evidence has revealed that Muse cells have a high transplantation survival rate. Yamada et al. (2018) found that the survival rate of Muse cells at 3 days post-transplantation in an acute myocardial infarction model was

approximately 14.5% compared with the survival rate of MSCs, which was close to zero. The anti-inflammatory function of Muse cells has also been investigated. Muse cells derived from adipose tissue can secrete high levels of TGF-β1 and can downregulate the secretion of proinflammatory cytokines in macrophages and splenocytes through the TGF-β1/pSMAD2 signaling pathway (Gimeno et al., 2017). Muse cells can also secrete IL-10 in more abundance than BMSCs and can reduce the inflammatory response in the intestine (Sun et al., 2020). Although Muse cells have been shown to partially improve hindlimb locomotor function in SD rats with spinal cord injury and to repair damaged tissues (Kajitani et al., 2021), the antineuroinflammatory capacity of Muse cells was only found to reduce the mRNA levels of TNF-α and iNOS (Suzuki et al., 2021). The mechanism that Muse cells use to regulate the CNS microenvironment has not been reported.

To explore this problem, we used LPS-stimulated microglia to simulate the inflammatory environment of the CNS and then cocultured the stimulated microglia with Muse cells. Microglia are important CNS immune cells and are sensitive to changes in the external environment, which affect the state of surrounding astrocytes and nerve cells and regulate the nearby immune response (Ransohoff, 2016; Mosser et al., 2017). Microglia can be divided into M1 and M2 cell types, which have different functions. Microglia can be activated to the M1 type by the presence of pathogens, abnormal stimulation, tissue damage, or danger-associated molecular pattern molecules including high mobility group protein B1, heat-shock proteins, histones, etc. These M1 activators trigger expression of various proinflammatory genes and proteins such as iNOS, IL-1β, TNF-α, and cyclooxygenase-1 (COX-1) (Tang et al., 2016; Rodriguez-Gomez et al., 2020), greatly increasing neuroinflammatory toxicity at the site of injury. In contrast, M2 microglia can express CD206, chitinase-3-like protein 3 (Ym1), Arg-1, and other proteins (Rezvan et al., 2020) and synthesize cytokines such as TGF-β, IL-4, and IL-10, which enables them to engulf damaged neuronal debris, suppress inflammatory responses, and promote neuronal repair and neural tissue regeneration (Tang et al., 2016). First, we examined the synthesis and secretion of inflammatory factors by microglia. We found that the transcription and secretion of TNF-α and IL-1β were significantly inhibited in the Muse group compared with the LPS group, and this suppression was superior to that of BMSCs. Muse cells and BMSCs both upregulated TGF-β expression. Muse cells dramatically increased the concentration of IL-10 secreted by microglia under LPS stimulation, which is in line with the results of another study (Sun et al., 2020), suggesting that Muse cells may mediate the microglial inflammatory response through the IL-10 pathway; however, the specific mechanism that controls this response has not yet been elucidated and requires further investigation. We also discovered that LPS-treated microglia could be stimulated to produce IL-10, which is inconsistent with the results of some studies that found a decrease in microglial IL-10 secretion in response to inflammation (Zhang et al., 2019; Sun et al., 2020). This may be because of changes in microglia status caused by the drug used to stimulate inflammation, the time of stimulation, and the microglia species, and these need to be explored further.

As changes in phenotype are often followed by functional modifications, as described above, we next examined the M1/M2 phenotype of microglia. In an inflammatory environment, microglia will transform from a branching-rich resting state to rounded or even hypertrophied M1 cells (Savage et al., 2019). In addition, iNOS is a recognized marker of M1 microglia; its overproduction can introduce significant toxicity to the neural microenvironment (Wierońska et al., 2021). Currently, reducing the presence of iNOS-positive microglia or directly knocking out the iNOS gene in microglia are two of the most important means to alleviate neuroinflammation (Mathy et al., 2021; Zhou et al., 2021a). During our detection of M1/M2 microglia markers, we discovered that Muse cells not only downregulated the transcription of the M1 microglia marker iNOS but also decreased the ratio of iNOS-positive cells in the total cell population and elevated the mRNA expression of Arg-1 and the protein level of CD206, both M2 markers. Combined with the previously discussed role of Muse cells in the expression of inflammatory factors in microglia, it was confirmed that Muse cells can regulate the phenotype of microglia in the inflammatory microenvironment, resulting in a decrease in the number of M1 microglia and an increase in the proportion of M2 microglia, and this effect is stronger than that for BMSCs.

TLR4 is a receptor widely expressed in cells in the CNS, such as microglia, neurons, and astrocytes, and is activated by many endogenous ligands. When TLR4 is stimulated, the downstream signaling ligand, such as MyD88, interleukin-1 receptor-associated kinases, or TNF receptor-associated factor 6, activates NF-κB, resulting in an inflammatory reaction that drives the release of proinflammatory cytokines such as TNF-α and IL-1β (Rahimifard et al., 2017). Similarly, the MAPK family (p38, JNK, and ERK) also comprises key signaling molecules involved in the inflammatory response in the CNS (Kim et al., 2019). To evaluate how Muse cells act on microglia, Muse cells were cocultured with microglia under LPS stimulation for 2 hours. Our results show that Muse cells inhibited the protein expression of TLR4 and MyD88 and the phosphorylation of p65, IκBα, and p38, whereas little effect was observed on JNK and ERK. This may be because Muse cells may only regulate the p38 MAPK signaling pathway and not the ERK and JNK signaling pathways. Alternatively, Muse cells might regulate key proteins in the MAPK pathway at different times after stimulation; we did not measure changes in ERK and JNK at all possible time points, and any changes over time need to be verified. Taken together, our results suggest that Muse cells might regulate microglia via the TLR4/MyD88/NF-κB and p38 MAPK signaling pathways.

There are some limitations to this study. First, we found that Muse cells can affect the NF-κB and MAPK pathways in microglia, but we have not yet verified whether the effect of Muse cells on microglia is mainly derived from these two pathways by testing the activation and inhibition of key proteins in these two pathways. Second, the anti-inflammatory effect of Muse cells *in vivo* has not yet been explored and needs to be investigated.

In conclusion, our findings outline the anti-inflammatory effect of Muse cells on microglia in an inflammatory environment for the first time. This effect of Muse cells is superior to that of BMSCs and may act through the TLR4/MyD88/NF-κB and p38 MAPK pathways. Our findings provide strong evidence for the further application of Muse cells for the treatment of CNS disease and injury. Future research should focus on the *in vivo* anti-inflammatory effect and mechanism of Muse cells as well as investigate the molecules that are secreted by Muse cells to generate their anti-inflammatory effect.

Acknowledgments: *We thank Mei-Mei Chen and He Liu (Department of Basic Medicine, Wuxi School of Medicine) for help with technical support.*

Author contributions: *Study design and manuscript writing: XC and XYY; human bone marrow acquisition: XSW; experiment implementation and material preparation: XYY, CCW, PD, YCL, YWS, YHS, YMH; statistical analysis: XYY. All authors approved the final version of the manuscript.*

Conflicts of interest: *The authors declare no conflicts of interest.*

Availability of data and materials: *All data generated or analyzed during this study are included in this published article and its supplementary information files.*

Open access statement: *This is an open access journal, and articles are distributed under the terms of the Creative Commons AttributionNonCommercial-ShareAlike 4.0 License, which allows others to remix, tweak, and build upon the work non-commercially, as long as appropriate credit is given and the new creations are licensed under the identical terms.*

Additional file:

Additional Figure 1: *Immunofluorescence staining to identify rat primary microglia.*

References

Bassett B, Subramaniyam S, Fan Y, Varney S, Pan H, Carneiro AMD, Chung CY (2021) Minocycline alleviates depression-like symptoms by rescuing decrease in neurogenesis in dorsal hippocampus via blocking microglia activation/phagocytosis. Brain Behav Immun 91:519-530.

Beigi Boroujeni F, Pasbakhsh P, Mortezaee K, Pirhajati V, Alizadeh R, Aryanpour R, Madadi S, Ragerdi Kashani I (2020) Intranasal delivery of SDF-1α-preconditioned bone marrow mesenchymal cells improves remyelination in the cuprizone-induced mouse model of multiple sclerosis. Cell Biol Int 44:499-511.

Colonna M, Butovsky O (2017) Microglia function in the central nervous system during health and neurodegeneration. Annu Rev Immunol 35:441-468.

Dezawa M (2018) Clinical trials of muse cells. In: Muse cells: endogenous reparative pluripotent stem cells (Dezawa M, ed), pp 305-307. Tokyo: Springer Japan.

Fawcett JW (2020) The struggle to make CNS axons regenerate: why has it been so difficult? Neurochem Res 45:144-158.

Fu Y, Xin Z, Liu B, Wang J, Wang J, Zhang X, Wang Y, Li F (2017) Platycodin D inhibits inflammatory response in LPS-stimulated primary rat microglia cells through activating LXRα-ABCA1 signaling pathway. Front Immunol 8:1929.

Gimeno ML, Fuertes F, Barcala Tabarrozzi AE, Attorressi AI, Cucchiani R, Corrales L, Oliveira TC, Sogayar MC, Labriola L, Dewey RA, Perone MJ (2017) Pluripotent nontumorigenic adipose tissue-derived Muse cells have immunomodulatory capacity mediated by transforming growth factor-β1. Stem Cells Transl Med 6:161-173.

Hu XC, Lu YB, Yang YN, Kang XW, Wang YG, Ma B, Xing S (2021) Progress in clinical trials of cell transplantation for the treatment of spinal cord injury: how many questions remain unanswered? Neural Regen Res 16:405-413.

Iseki M, Kushida Y, Wakao S, Akimoto T, Mizuma M, Motoi F, Asada R, Shimizu S, Unno M, Chazenbalk G, Dezawa M (2017) Muse cells, nontumorigenic pluripotent-like stem cells, have liver regeneration capacity through specific homing and cell replacement in a mouse model of liver fibrosis. Cell Transplant 26:821-840.

Kajitani T, Endo T, Iwabuchi N, Inoue T, Takahashi Y, Abe T, Niizuma K, Tominaga T (2021) Association of intravenous administration of human Muse cells with deficit amelioration in a rat model of spinal cord injury. J Neurosurg Spine 34:648-655.

Kim JE, Park H, Choi SH, Kong MJ, Kang TC (2019) Roscovitine attenuates microglia activation and monocyte infiltration via p38 MAPK inhibition in the rat frontoparietal cortex following status epilepticus. Cells 8:746.

Kobashi S, Terashima T, Katagi M, Nakae Y, Okano J, Suzuki Y, Urushitani M, Kojima H (2020) Transplantation of M2-deviated microglia promotes recovery of motor function after spinal cord injury in mice. Mol Ther 28:254-265.

Kuroda Y, Kitada M, Wakao S, Nishikawa K, Tanimura Y, Makinoshima H, Goda M, Akashi H, Inutsuka A, Niwa A, Shigemoto T, Nabeshima Y, Nakahata T, Nabeshima Y, Fujiyoshi Y, Dezawa M (2010) Unique multipotent cells in adult human mesenchymal cell populations. Proc Natl Acad Sci U S A 107:8639-8643.

Li S, Guan H, Zhang Y, Li S, Li K, Hu S, Zuo E, Zhang C, Zhang X, Gong G, Wang R, Piao F (2021) Bone marrow mesenchymal stem cells promote remyelination in spinal cord by driving oligodendrocyte progenitor cell differentiation via TNFalpha/RelB-Hes1 pathway: a rat model study of 2,5-hexanedione-induced neurotoxicity. Stem Cell Res Ther 12:436.

Lin M, Liu X, Zheng H, Huang X, Wu Y, Huang A, Zhu H, Hu Y, Mai W, Huang Y (2020) IGF-1 enhances BMSC viability, migration, and anti-apoptosis in myocardial infarction via secreted frizzled-related protein 2 pathway. Stem Cell Res Ther 11:22.

Liu W, Wang Y, Gong F, Rong Y, Luo Y, Tang P, Zhou Z, Zhou Z, Xu T, Jiang T, Yang S, Yin G, Chen J, Fan J, Cai W (2019) Exosomes derived from bone mesenchymal stem cells repair traumatic spinal cord injury by suppressing the activation of A1 neurotoxic reactive astrocytes. J Neurotrauma 36:469-484.

Livak KJ, Schmittgen TD (2001) Analysis of relative gene expression data using real-time quantitative PCR and the 2(-Delta Delta C(T)) Method. Methods 25:402-408.

Lo Furno D, Mannino G, Giuffrida R (2018) Functional role of mesenchymal stem cells in the treatment of chronic neurodegenerative diseases. J Cell Physiol 233:3982-3999.

Luo Z, Lin J, Sun Y, Wang C, Chen J (2021) Bone marrow stromal cell-derived exosomes promote muscle healing following contusion through macrophage polarization. Stem Cells Dev 30:135-148.

Mathy NW, Burleigh O, Kochvar A, Whiteford ER, Behrens M, Marta P, Tian C, Gong AY, Drescher KM, Steyger PS, Chen XM, Shibata A (2021) A novel long intergenic non-coding RNA, Nostrill, regulates iNOS gene transcription and neurotoxicity in microglia. J Neuroinflammation 18:16.

Mithaiwala MN, Santana-Coelho D, Porter GA, O'Connor JC (2021) Neuroinflammation and the kynurenine pathway in CNS disease: molecular mechanisms and therapeutic implications. Cells 10:1548.

Mosser CA, Baptista S, Arnoux I, Audinat E (2017) Microglia in CNS development: Shaping the brain for the future. Prog Neurobiol 149-150:1-20.

Neirinckx V, Cantinieaux D, Coste C, Rogister B, Franzen R, Wislet-Gendebien S (2014) Concise review: Spinal cord injuries: how could adult mesenchymal and neural crest stem cells take up the challenge? Stem Cells 32:829-843.

Rahimifard M, Maqbool F, Moeini-Nodeh S, Niaz K, Abdollahi M, Braidy N, Nabavi SM, Nabavi SF (2017) Targeting the TLR4 signaling pathway by polyphenols: A novel therapeutic strategy for neuroinflammation. Ageing Res Rev 36:11-19.

Ransohoff RM (2016) A polarizing question: do M1 and M2 microglia exist? Nat Neurosci 19:987-991.

Rezvan M, Meknatkhah S, Hassannejad Z, Sharif-Alhoseini M, Zadegan SA, Shokraneh F, Vaccaro AR, Lu Y, Rahimi-Movaghar V (2020) Time-dependent microglia and macrophages response after traumatic spinal cord injury in rat: a systematic review. Injury 51:2390-2401.

Rodriguez-Gomez JA, Kavanagh E, Engskog-Vlachos P, Engskog MKR, Herrera AJ, Espinosa-Oliva AM, Joseph B, Hajji N, Venero JL, Burguillos MA (2020) Microglia: Agents of the CNS pro-inflammatory response. Cells 9:1717.

Savage JC, Carrier M, Tremblay ME (2019) Morphology of microglia across contexts of health and disease. Methods Mol Biol 2034:13-26.

Schneider CA, Rasband WS, Eliceiri KW (2012) NIH Image to ImageJ: 25 years of image analysis. Nat Methods 9:671-675.

Shichinohe H, Kuroda S, Sugiyama T, Ito M, Kawabori M, Nishio M, Takeda Y, Koike T, Houkin K (2011) Biological features of human bone marrow stromal cells (hBMSC) cultured with animal protein-free medium-safety and efficacy of clinical use for neurotransplantation. Transl Stroke Res 2:307-315.

Singh SS, Rai SN, Birla H, Zahra W, Rathore AS, Singh SP (2020) NF-κB-Mediated Neuroinflammation in Parkinson's Disease and Potential Therapeutic Effect of Polyphenols. Neurotox Res 37:491-507.

Sun C, Zhang AD, Chen HH, Bian J, Liu ZJ (2021) Magnet-targeted delivery of bone marrow-derived mesenchymal stem cells improves therapeutic efficacy following hypoxic-ischemic brain injury. Neural Regen Res 16:2324-2329.

Sun D, Yang L, Cao H, Shen ZY, Song HL (2020) Study of the protective effect on damaged intestinal epithelial cells of rat multilineage-differentiating stress-enduring (Muse) cells. Cell Biol Int 44:549-559.

Suzuki T, Sato Y, Kushida Y, Tsuji M, Wakao S, Ueda K, Imai K, Iitani Y, Shimizu S, Hida H, Temma T, Saito S, Iida H, Mizuno M, Takahashi Y, Dezawa M, Borlongan CV, Hayakawa M (2021) Intravenously delivered multilineage-differentiating stress enduring cells dampen excessive glutamate metabolism and microglial activation in experimental perinatal hypoxic ischemic encephalopathy. J Cereb Blood Flow Metab 41:1707-1720.

Tang JJ, Wang MR, Dong S, Huang LF, He QR, Gao JM (2021) 1,10-Seco-Eudesmane sesquiterpenoids as a new type of anti-neuroinflammatory agents by suppressing TLR4/NF-κB/MAPK pathways. Eur J Med Chem 224:113713.

Tang Y, Le W (2016) Differential roles of M1 and M2 microglia in neurodegenerative diseases. Mol Neurobiol 53:1181-1194.

Uchida H, Morita T, Niizuma K, Kushida Y, Kuroda Y, Wakao S, Sakata H, Matsuzaka Y, Mushiake H, Tominaga T, Borlongan CV, Dezawa M (2016) Transplantation of unique subpopulation of fibroblasts, Muse cells, ameliorates experimental stroke possibly via robust neuronal differentiation. Stem Cells 34:160-173.

Wierońska JM, Cieślik P, Kalinowski L (2021) Nitric oxide-dependent pathways as critical factors in the consequences and recovery after brain ischemic hypoxia. Biomolecules 11:1097.

Wu H, Zheng J, Xu S, Fang Y, Wu Y, Zeng J, Shao A, Shi L, Lu J, Mei S, Wang X, Guo X, Wang Y, Zhao Z, Zhang J (2021) Mer regulates microglial/macrophage M1/M2 polarization and alleviates neuroinflammation following traumatic brain injury. J Neuroinflammation 18:2.

Xiong LL, Liu F, Lu BT, Zhao WL, Dong XJ, Liu J, Zhang RP, Zhang P, Wang TH (2017) Bone marrow mesenchymal stem-cell transplantation promotes functional improvement associated with CNTF-STAT3 activation after hemi-sectioned spinal cord injury in tree shrews. Front Cell Neurosci 11:172.

Xu M, Wang J, Zhang X, Yan T, Wu B, Bi K, Jia Y (2020) Polysaccharide from Schisandra chinensis acts via LRP-1 to reverse microglia activation through suppression of the NF-κB and MAPK signaling. J Ethnopharmacol 256:112798.

Yamada Y, Wakao S, Kushida Y, Minatoguchi S, Mikami A, Higashi K, Baba S, Shigemoto T, Kuroda Y, Kanamori H, Amin M, Kawasaki M, Nishigaki K, Taoka M, Isobe T, Muramatsu C, Dezawa M, Minatoguchi S (2018) S1P-S1PR2 axis mediates homing of muse cells into damaged heart for long-lasting tissue repair and functional recovery after acute myocardial infarction. Circ Res 122:1069-1083.

Yang LK, Lu L, Yue J, Wang XS, Qi JY, Yang F, Liu SB (2021) Activation of microglial G-protein-coupled receptor 30 protects neurons against excitotoxicity through NF-κB/MAPK pathways. Brain Res Bull 172:22-30.

Yang QQ, Zhou JW (2019) Neuroinflammation in the central nervous system: Symphony of glial cells. Glia 67:1017-1035.

Yu J, Liu XL, Cheng QG, Lu SS, Xu XQ, Zu QQ, Liu S (2016) G-CSF and hypoxic conditioning improve the proliferation, neural differentiation and migration of canine bone marrow mesenchymal stem cells. Exp Ther Med 12:1822-1828.

Zhan J, Li X, Luo D, Hou Y, Hou Y, Chen S, Xiao Z, Luan J, Lin D (2020) Polydatin promotes the neuronal differentiation of bone marrow mesenchymal stem cells in vitro and in vivo: Involvement of Nrf2 signalling pathway. J Cell Mol Med 24:5317-5329.

Zhang J, Zheng Y, Luo Y, Du Y, Zhang X, Fu J (2019) Curcumin inhibits LPS-induced neuroinflammation by promoting microglial M2 polarization via TREM2/ TLR4/ NF-κB pathways in BV2 cells. Mol Immunol 116:29-37.

Zhang L, Liu Y, Wang S, Long L, Zang Q, Ma J, Yu L, Jia G (2021) Vagus nerve stimulation mediates microglia M1/2 polarization via inhibition of TLR4 pathway after ischemic stroke. Biochem Biophys Res Commun 577:71-79.

Zhou T, Liu Y, Yang Z, Ni B, Zhu X, Huang Z, Xu H, Feng Q, Lin X, He C, Liu X (2021a) IL-17 signaling induces iNOS+ microglia activation in retinal vascular diseases. Glia 69:2644-2657.

Zhou X, Zhang J, Li Y, Cui L, Wu K, Luo H (2021b) Astaxanthin inhibits microglia M1 activation against inflammatory injury triggered by lipopolysaccharide through down-regulating miR-31-5p. Life Sci 267:118943.

C-Editor: Zhao M; S-Editor: Li CH; L-Editors: McRae M, Li CH, Song LP; T-Editor: Jia Y

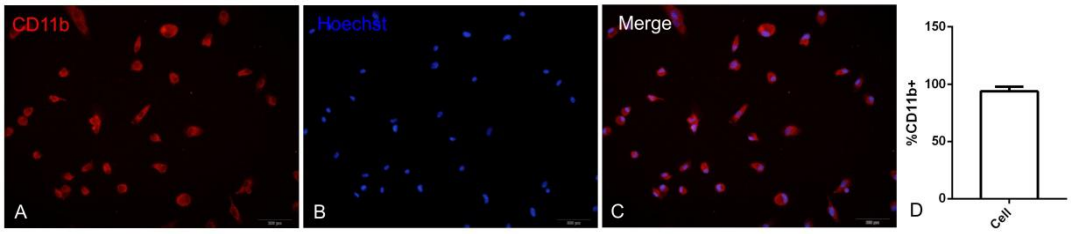

Additional Figure 1 Immunofluorescence staining to identify rat primary microglia.
(A–C) Rat primary microglia were stained with CD11b (red) and Hoechst 33342 (blue). Scale bars: 200 μm. (D) Percentage of CD11b-positive cells.